J|A|C|S
ARTICLES
Published on Web 05/18/2007

Two Classes of Alongside Charge-Transfer Interactions Defined in One [2]Catenane

Sune Nygaard,[†,‡] Stinne W. Hansen,[†] John C. Huffman,[‡] Frank Jensen,[†] Amar H. Flood,*[,‡] and Jan O. Jeppesen*[,†]

Contribution from the Department of Physics and Chemistry, University of Southern Denmark, Odense University, Campusvej 55, 5230, Odense M, Denmark and Department of Chemistry, University of Indiana—Bloomington, 800 East Kirkwood Avenue, Bloomington, Indiana 47405

Received December 27, 2006; E-mail: aflood@indiana.edu; joj@ifk.sdu.dk

Abstract: A [2]catenane, which incorporates hydroquinone (HQ) and a sterically bulky tetrathiafulvalene (TTF) into a bismacrocycle, has been designed to probe the alongside charge-transfer (CT) interactions taking place between a TTF unit and one of the bipyridinium moieties in the tetracationic cyclophane cyclobis(paraquat-*p*-phenylene) ($CBPQT^{4+}$). A template-directed strategy employs the HQ unit as the primary template for formation of the tetracationic cyclophane $CBPQT^{4+}$, affording the desired [2]catenane structure but as an uncharacteristic green solid. The X-ray crystal structure and detailed ^{13}C NMR assignments have identified a stereoselective preference for catenation about the *cis* isomer. The ^{1}H NMR spectroscopy, electrochemistry, and X-ray crystallography all confirm that the $CBPQT^{4+}$ cyclophane encircles the HQ unit, thereby defining a structure which would normally determine a red color. The visible−NIR region of the absorption spectrum displays a band at ~740 nm that is unambiguously assigned to a TTF → $CBPQT^{4+}$ CT transition on the basis of resonance Raman spectroscopy using 785 nm excitation. The profile of the CT band changes depending on the ratio of the *cis*- to *trans*-TTF isomers in the [2]catenane for which the molar absorptivity of each isomer is estimated to be significantly different at $\epsilon_{max} = 380$ and 3690 M^{-1} cm^{-1}, respectively. Molecular modeling studies confirmed that the observed difference in the absorption spectroscopic profile can be accounted for by both a better overlap of the HOMO(TTF) and LUMO+1($CBPQT^{4+}$) as well as a more stable face-to-face ($\pi\cdots\pi$) conformation in the *trans* isomer compared to the edge-to-face *cis* isomer of the [2]catenane. The latter is arranged for π-orbital overlap through the sulfur atoms of the TTF unit, thereby defining an [S$\pi\cdots\pi$] interaction.

Introduction

Through the last couple of decades a wide range of different interlocked structures,[1] macromolecular assemblies,[2] and charge-transfer (CT) conducting salts[3] have been constructed by employing the concepts of self-assembly[4] and self-organization.[4,5] Of particular note are the fabrication of structures with increasing complexity such as catenanes[6] and rotaxanes,[6a,b,7] as well as molecular lifts,[8] unidirectional motion systems,[9] and light-harvesting entities.[10] These structures emerge from the control over a range of noncovalent interactions including edge-

[†] University of Southern Denmark.

[‡] University of Indiana—Bloomington.

(1) (a) Ashton, P. R.; Campbell, P. J.; Chrystal, E. J. T.; Glink, P. T.; Menzer, S.; Philp, D.; Spencer, N.; Stoddart, J. F.; Williams, D. J. *Angew. Chem., Int. Ed. Engl.* **1995**, *34*, 1865−1869. (b) Weck, M.; Mohr, B.; Sauvage, J.-P.; Grubbs, R. H. *J. Org. Chem.* **1999**, *64*, 5463−5471. (c) Seel, C.; Vögtle, F. *Chem. Eur. J.* **2000**, *6*, 21−24. (d) Gunter, M. J.; Bampos, N.; Johnstone, K. D.; Sanders, J. K. M. *New J. Chem.* **2001**, *25*, 166−173. (e) Furusho, Y.; Oku, T.; Hasegawa, T.; Tsuboi, A.; Kihara, N.; Takata, T. *Chem. Eur. J.* **2003**, *9*, 2895−2903. (f) Fuller, A.-M.; Leigh, D. A.; Lusby, P. J.; Oswald, I. D. H.; Parsons, S.; Walker, D. B. *Angew. Chem., Int. Ed.* **2004**, *43*, 3914−3918. (g) Furusho, Y.; Sasabe, H.; Natsui, D.; Murakawa, K.; Takata, T.; Harada, T. *Bull. Chem. Soc. Jpn.* **2004**, *77*, 179−185.

(2) (a) Gong, C.; Gibson, H. W. *Macromol. Chem. Phys.* **1998**, *199*, 1801−1806. (b) Percec, V.; Cho, W.-D.; Ungar, G.; Yeardley, J. P. *J. Am. Chem. Soc.* **2001**, *123*, 1302−1315. (c) Schenning, A. P. H. J.; Kilbinger, A. F. M.; Biscarini, F.; Cavallini, M.; Cooper, H. J.; Derrick, P. J.; Feast, W. J.; Lazzaroni, R.; Leclere, Ph.; McDonell, L. A.; Meijer, E. W.; Meskers, S. C. J. *J. Am. Chem. Soc.* **2001**, *124*, 1269−1275. (d) Wilson, A. J.; Masuda, M.; Sijbesma, R. P.; Meijer, E. W. *Angew. Chem., Int. Ed.* **2005**, *44*, 2275−2279. (e) Pantos, G. D.; Pengo, P.; Sanders, J. K. M. *Angew. Chem., Int. Ed.* **2006**, *45*, 1−5.

(3) (a) Torrance, J. B.; Mayerle, J. J.; Lee, V. Y.; Bechgaard, K. *J. Am. Chem. Soc.* **1979**, *101*, 4747−4748. (b) Akutsu, H.; Kato, K.; Ojima, E.; Kobayashi, H.; Tanaka, H.; Kobayashi, A.; Cassoux, P. *Phys. Rev. B* **1998**, *58*, 9294−9302. (c) Akustu-Sato, A.; Akutsu, H.; Turner, S. S.; Day, P.; Probert, M. R.; Howard, J. A. K.; Akutagawa, T.; Takeda, S.; Nakamura, T.; Mori, T. *Angew. Chem., Int. Ed.* **2005**, *44*, 292−295.

(4) (a) Lehn, J. M. *Angew. Chem., Int. Ed. Engl.* **1990**, *29*, 1304−1319. (b) Philp, D.; Stoddart, J. F. *Angew. Chem., Int. Ed. Engl.* **1996**, *35*, 1154−1196. (c) Claessens, C. G.; Stoddart, J. F. *J. Phys. Org. Chem.* **1997**, *10*, 254−272. (d) Krische, M. J.; Lehn, J. M. *Mol. Self-Assembly Struct. Bonding* **2000**, *96*, 3−29. (e) Bowden, N. B.; Weck, M.; Choi, I. S.; Whitesides, G. M. *Acc. Chem. Res.* **2001**, *34*, 231−238. (f) Lehn, J. M. *Rep. Prog. Phys.* **2004**, *67*, 249−265.

(5) (a) Lehn, J. M. *Supramolecular Chemistry: Concepts and Perspectives*; VCH: Weinheim, 1995. (b) Lehn, J. M. *Proc. Natl Acad. Sci. U.S.A.* **2002**, *99*, 4763−4768. (c) Lehn, J. M. *Science* **2002**, *295*, 2400−2403.

(6) (a) Schill, G. *Catenanes, Rotaxanes and Knots*; Academic: New York, 1971. (b) *Molecular Catenanes, Rotaxanes and Knots*; Sauvage, J.-P., Dietrich-Buchecker, C., Eds.; VCH-Wiley: Weinheim, 1999. (c) Li, Z.-T.; Stein, P. C.; Becher, J.; Jensen, D.; Mørk, P.; Svenstrup, N. *Chem. Eur. J* **1996**, *2*, 624−633. (d) Li, Z.-T.; Becher, J. *Synlett* **1997**, 557−560. (e) Becher, J.; Li, Z.-T.; Blanchard, P.; Svenstrup, N.; Lau, J.; Nielsen, M. B.; Leriche, P. *Pure Appl. Chem.* **1997**, *69*, 465−470. (f) Nielsen, M. B.; Li, Z.-T.; Becher, J. *J. Mater. Chem.* **1997**, *7*, 1175−1187. (g) Lau, J.; Nielsen, M. B.; Thorup, N.; Cava, M. P.; Becher, J. *Eur. J. Org. Chem.* **1999**, 3335−3341. (h) Ballardini, R.; Balzani, V.; Fabio, A. D.; Gandolfi, M. T.; Becher, J.; Lau, J.; Nielsen, M. B.; Stoddart, J. F. *New J. Chem.* **2001**, *25*, 293−298. (i) Liu, Y.; Bonvallet, P. A.; Vignon, S. A.; Khan, S. I.; Stoddart, J. F. *Angew. Chem., Int. Ed.* **2005**, *44*, 3050−3055. (j) Guidry, E. N.; Cantrill, S. J.; Stoddart, J. F.; Grubbs, R. H. *Org. Lett.* **2005**, *7*, 2129−2132. (k) Leigh, D. A.; Lusby, P. J.; Slawin, A. M. Z.; Walker, D. B *Angew. Chem., Int. Ed.* **2005**, *44*, 4557−4564.

 10.1021/ja069047w CCC: $37.00

to-face [CH···π] interactions,[11] hydrogen bonding, and CT interactions.[12] One class of CT interactions occurs when the central cavity of a cyclophane is blocked, thereby forcing the π-donor and -acceptor pair to interact in an alongside[13] manner. These alongside interactions can be further subdivided based upon the relative orientation of the donor/acceptor pair into face-to-face[11c,13] and edge-to-face of which the latter arise in specific situations.[14] For both synthetic purposes and machine-like functionality, a significant number of the more complex interlocked structures have been relying on the sum of the noncovalent interactions that occur between the tetracationic π-electron-deficient cyclophane[15] cyclobis(paraquat-*p*-phenylene) ($CBPQT^{4+}$) serving as a host and the efficient π-electron-rich guests, such as dioxynaphthalene (DNP),[6c,d,e,16] tetrathiafulvalene (TTF),[16b,d,17] monopyrrolotetrathiafulvalene (MPTTF),[18] and 1,4-dihydroquinone (HQ) units.[6c,f,g,16a] Once the guests are accommodated inside the $CBPQT^{4+}$ cyclophane's cavity, a characteristic color is observed that originates from the CT interaction between the guest and the host. It is well known that aromatic entities such as DNP and HQ give rise to a distinct red or purple color, respectively,[8a,18b−d,19] originating from a weak CT electronic absorption band at ∼500 nm ($\epsilon \approx$ 100's M^{-1} cm^{-1}), whereas inclusion of various TTF units invariably results in formation of a more intense characteristic CT band in the 750−850 nm ($\epsilon \approx 1000$'s M^{-1} cm^{-1}) region.[18,20] The fact that the CT interaction between the $CBPQT^{4+}$ cyclophane and the π-electron-rich guests gives rise to such well-characterized and well-assigned CT bands has determined that the analysis of CT bands has been both ubiquitous and of prime importance particularly in cases when the structures and dynamics of more complex interlocked molecules, such as bistable [2]rotaxanes, have been examined.[18]

Most [2]catenanes and [2]rotaxanes prepared so far have been characterized[16−19,21] by a high degree of flexibility on account of the fact that the various π-electron-rich units in the interlocked systems have historically been linked by flexible poly(ethylene glycol) (PEG) chains, a feature which has conferred a high degree of folding and thereby allowed for various conformations to exist in solution as well as in more condensed phases.[10c,22] Building on the inherent flexibility of the interlocked compounds, it has long been known that the dynamic nature of nondegenerate two-station [2]catenanes and [2]rotaxanes can lead to competing co-conformations in which some of them can be surprisingly stable.[21] In particular, [2]rotaxanes[18b−d,21,23] have been found to exist in co-conformations in which the tetracationic cyclophane is positioned on the weakest π-electron donor. In such examples it was observed that the $CBPQT^{4+}$ cyclophane interacts in an *alongside manner* with the stronger π-electron donor, confirmed by analysis[18c,24] of the UV−vis−NIR absorp-

(7) (a) Amabilino, D. B.; Stoddart, J. F. *Chem. Rev.* **1995**, *95*, 2725−2828. (b) Vögtle, F.; Dunnwald, T.; Schmidt, T. *Acc. Chem. Res.* **1996**, *29*, 451−460. (c) Breault, G. A.; Hunter, C. A.; Mayers, P. C. *Tetrahedron* **1999**, *55*, 5265−5293. (d) Hubin, T. J.; Kolchinski, A. G.; Vance, A. L.; Busch, D. H. *Adv. Supramol. Chem.* **1999**, *5*, 237−357. (e) Raehm, L.; Hamilton, D. G.; Sanders, J. K. M. *Synlett* **2002**, 1743−1761. (f) Stoddart, J. F.; Tseng, H.-R. *Proc. Natl. Acad. Sci. U.S.A.* **2002**, *99*, 4797−4800. (g) Gatti, G.; León, S.; Wong, J. K. Y.; Bottari, G.; Altieri, A.; Morales, M. A. F.; Teat, S. J.; Frochot, C.; Leigh, D. A.; Brouwer, A. M.; Zerbetto, F. *Proc. Natl. Acad. Sci. U.S.A.* **2003**, *100*, 10−14. (h) Leigh, D. A.; Pérez, E. M. *Chem. Commun.* **2004**, 2262−2263. (i) Sauvage, J.-P. *Chem. Commun.* **2005**, 1507−1510. (j) Marlin, D. S.; Gonzalez, C.; Leigh, D. A.; Slawin, A. M. Z. *Angew. Chem., Int. Ed.* **2006**, *45*, 77−83. (k) Dichtel, W. R.; Miljanic, O. S.; Spruell, J. M.; Heath, J. M.; Stoddart, J. F. *J. Am. Chem. Soc.* **2006**, *128*, 10388−10390. (l) Nygaard, S.; Liu, Y.; Stein, P. C.; Flood, A. H.; Jeppesen, J. O. *Adv. Funct. Mater.* **2007**, *17*, 751−762.

(8) (a) Badjic, J. D.; Balzani, V.; Credi, A.; Silvi, S.; Stoddart, J. F. *Science* **2004**, *303*, 1845−1849. (b) Badjic, J. D.; Ronconi, C. M.; Stoddart, J. F.; Balzan, V.; Silvi, S.; Credi, A. *J. Am. Chem. Soc* **2006**, *128*, 1489−1499.

(9) Leigh, D. A.; Wong, J. K. Y.; Dehez, F.; Zerbetto, F. *Nature* **2003**, *424*, 174−179.

(10) (a) Saha, S.; Johansson, E.; Flood, A. H.; Tseng, H.-R.; Zink, J. I.; Stoddart, J. F. *Chem. Eur. J.* **2005**, *11*, 5796−5804. (b) Guldi, D. M. *Chem. Soc. Rev.* **2002**, *31*, 22−36. (c) Braunschweig, A. B.; Northrop, B. H.; Stoddart, J. F. *J. Mater. Chem.* **2006**, *16*, 32−44.

(11) (a) Nishio, M.; Umezawa, Y.; Hirota, M.; Takeuchi, Y. *Tetrahedron* **1995**, *51*, 8665−8701. (b) Adams, H.; Carver, F. J.; Hunter, C. A.; Morales, J. C.; Seward, E. M. *Angew. Chem., Int. Ed. Engl.* **1996**, *35*, 1542−1544. (c) Guldi, D. M.; Luo, C.; Prato, M.; Troisi, A.; Zerbetto, F.; Scheloske, M.; Dietel, A.; Bauer, W.; Hirsch, A. *J. Am. Chem. Soc.* **2001**, *123*, 9166−9167. (d) Ma, B.-Q.; Coppens, P. *Chem. Commun.* **2003**, 2290−2291.

(12) For an introduction and overview over the wide array of weak noncovalent interactions please refer to the dollowing refs: (a) Hunter, C. A.; Sanders, J. K. M. *J. Am. Chem. Soc.* **1990**, *112*, 5525−5534. (b) Steed, J. W.; Atwood, J. L. *Supramolecular Chemistry*; John Wiley & Sons, Ltd.: New York, 2000. (c) Schmittel, M.; Kalsani, V. *Top. Curr. Chem.* **2005**, *245*, 1−53.

(13) Menzer, S.; White, A. J. P.; Williams, D. J.; Belohradsky, M.; Hamers, C.; Raymo, F. M.; Shipway, A. N.; Stoddart, J. F. *Macromolecules* **1998**, *31*, 295−307 and references therein.

(14) (a) For edge-to-face arrangements between TTF and $CBPQT^{4+}$, see: Li, Z.-T.; Becher, J. *Chem. Commun.* **1996**, 639−640 and ref 6e. (b) For an early identification of an end-on, edge-to-face CT interaction between a TTF unit and $CBPQT^{4+}$, see refs 6c,f. (c) For edge-to-face CT interactions involving heterocyclic nitrogen and diazapyrenium cations, see: Becker, H.-C.; Broo, A.; Nordén, B. *J. Phys. Chem.* **1997**, *101*, 8853−8860. (d) For inter-TTF edge-to-face arrangements of a neutral TTF dimer and the CT interactions of a radical cation, see: Batsanov, A. S.; John, D. E.; Bryce, M. R.; Howard, J. A. K. *Adv. Mater.* **1998**, *10*, 1360−1363. (e) For [CH···π] edge-to-face CT interactions involving pyridinium cations, see: Acharya, P.; Plashkevych, O.; Morita, C.; Yamada, S.; Chattopadhyaya, J. *J. Org. Chem.* **2003**, *68*, 1529−1538.

(15) (a) Anelli, P.-L. et al. *J. Am. Chem. Soc.* **1992**, *114*, 193−218. (b) Asakawa, M.; Dehaen, W.; L'abbé, G.; Menzer, S.; Nouwen, J.; Raymo, F. M.; Stoddart, J. F.; Williams, D. J. *J. Org. Chem.* **1996**, *61*, 9591−9595.

(16) (a) Asakawa, M.; Ashton, P. R.; Balzani, V.; Brown, C. L.; Credi, A.; Matthews, O. A.; Newton, S. P.; Raymo, F. M.; Shipway, A. N.; Spencer, N.; Quick, A.; Stoddart, J. F.; White, A. J. P.; Williams, D. J. *Chem. Eur. J.* **1999**, *5*, 860−875. (b) Liu, Y.; Flood, A. H.; Bonvallet, P. A.; Vignon, S. A.; Northrop, B. H.; Tseng, H.-R.; Jeppesen, J. O.; Huang, T. J.; Brough, B.; Baller, M.; Magonov, S.; Solares, S. D.; Goddard, W. A.; Ho, C.-M.; Stoddart, J. F. *J. Am. Chem. Soc.* **2005**, *127*, 9745−9759. (c) Liu, Y.; Bonvallet, P. A.; Vignon, S. A.; Khan, S. I.; Stoddart, J. F. *Angew. Chem., Int. Ed.* **2005**, *44*, 3050−3055. (d) Liu, Y.; Saha, S.; Vignon, S. A.; Flood, A. H.; Stoddart, J. F. *Synthesis* **2005**, *19*, 3437−3445.

(17) (a) Yamamoto, T.; Tseng, H.-R.; Stoddart, J. F.; Balzani, V.; Credi, A.; Marchioni, F.; Venturi, M. *Collect. Czech. Chem. Commun.* **2003**, *68*, 1488−1514. (b) Tseng, H.-R.; Vignon, S. A.; Stoddart, J. F. *Angew. Chem., Int. Ed.* **2003**, *43*, 1491−1495. (c) Tseng, H.-R.; Vignon, S. A.; Celestre, P. C.; Perkins, J.; Jeppesen, J. O.; Di, Fabio, A.; Ballardini, R.; Gandolfi, M. T.; Venturi, M.; Balzani, V.; Stoddart, J. F. *Chem. Eur. J.* **2004**, *10*, 155−172.

(18) (a) Jeppesen, J. O.; Perkins, J.; Becher, J.; Stoddart, J. F. *Org. Lett.* **2000**, *2*, 3547−3550. (b) Jeppesen, J. O.; Perkins, J.; Becher, J.; Stoddart, J. F. *Angew. Chem., Int. Ed.* **2001**, *40*, 1216−1221. (c) Jeppesen, J. O.; Nielsen, K. A.; Perkins, J.; Vignon, S. A.; Di Fabio, A.; Ballardini, R.; Gandolfi, M. T.; Venturi, M.; Balzani, V.; Becher, J.; Stoddart, J. F. *Chem. Eur. J.* **2003**, *9*, 2982−3007. (d) Jeppesen, J. O.; Nygaard, S.; Vignon, S. A.; Stoddart, J. F. *Eur. J. Org. Chem.* **2005**, 196−220. (e) Nygaard, S.; Laursen, B. W.; Flood, A. H.; Hansen, C. N.; Jeppesen, J. O. *Chem. Commun.* **2006**, *2*, 144−146. (f) Nygaard, S.; Leung, K. C.-F.; Aprahamian, I.; Ikeda, T.; Saha, S.; Laursen, B. W.; Kim, S.-Y.; Hansen, S. W.; Stein, P. C.; Flood, A. H.; Stoddart, J. F.; Jeppesen, J. O. *J. Am. Chem. Soc.* **2007**, *129*, 960−970.

(19) Jeppesen, J. O.; Becher, J.; Stoddart, J. F. *Org. Lett.* **2002**, *4*, 557−560.

(20) (a) Devonport, W.; Blower, M. A.; Bryce, M. R.; Goldenberg, L. M. *J. Org. Chem.* **1997**, *62*, 885−887. (b) Nielsen, M. B.; Jeppesen, J. O.; Lau, J.; Lomholt, C.; Damgaard, D.; Jacobsen, J. P.; Becher, J.; Stoddart, J. F. *J. Org. Chem.* **2001**, *66*, 3559−3563. (c) Nyggard, S.; Hansen, C. N.; Jeppesen, J. O. *J. Org. Chem.* **2007**, *72*, 1617−1626.

(21) Choi, J. W.; Flood, A. H.; Steuerman, D. W.; Nygaard, S.; Braunschweig, A. B.; Moonen, N. N. P.; Laursen, B. W.; Luo, Y.; DeIonno, E.; Peters, A. J.; Jeppesen, J. O.; Xu, K.; Stoddart, J. F.; Heath, J. R. *Chem. Eur. J.* **2006**, *12*, 261−279.

(22) (a) Lee, I. C.; Frank, C. W.; Yamamoto, T.; Tseng, H.-R.; Flood, A. H.; Stoddart, J. F.; Jeppesen, J. O. *Langmuir* **2004**, *20*, 5809−5828. (b) Nørgaard, K.; Jeppesen, J. O.; Laursen, B. W.; Simonsen, J. B.; Weygand, M.; Kjaer, J. K.; Stoddart, J. F.; Bjørnholm, T. *J. Phys. Chem. B* **2005**, *109*, 1063−1066. (c) Nørgaard, K.; Laursen, B. W.; Nygaard, S.; Kjaer, K.; Tseng, H.-R.; Flood, A. H.; Stoddart, J. F.; Bjørnholm, T. *Angew. Chem., Int. Ed.* **2005**, *44*, 7035−7039. (d) Mendes, P. M.; Lu, W. X.; Tseng, H.-R.; Shinder, S.; Iijima, T.; Miyaji, M.; Knobler, C. M.; Stoddart, J. F. *J. Phys. Chem. B* **2006**, *110*, 3845−3848.

(23) Laursen, B. W.; Nygaard, S.; Jeppesen, J. O.; Stoddart, J. F. *Org. Lett.* **2004**, *6*, 4167−4170.

(24) Jeppesen, J. O.; Vignon, S. A.; Stoddart, J. F. *Chem. Eur. J.* **2003**, *9*, 4611−4625.

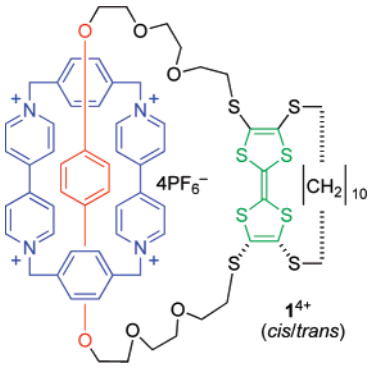

Figure 1. Molecular structure of the [2]catenane **1**·4PF_6.

tion spectroscopy, whereas it is usually assumed that the $CBPQT^{4+}$ cyclophane will exclusively encircle the most π-electron-rich unit. These findings can be rationalized by taking into account that the favored co-conformation is determined by host−guest $\pi-\pi$ stacking as well as by a wide array of weaker [CH···π], [CH···O], and alongside CT interactions. These noncovalent bonding interactions can all be accommodated when there is sufficient flexibility in the interlocked molecule. In the drive toward exercising greater control and providing a deeper understanding of these weak noncovalent interactions,[12] all insights that can ultimately lead to the rational utilization of the least studied alongside interaction are considered to be of paramount importance for the development of increasingly complex interlocked systems. In order to investigate and understand the alongside interaction involving the $CPBQT^{4+}$ cyclophane and a strong donor we constructed a [2]catenane **1**·4PF_6 (Figure 1) composed by a TTF unit which, for steric reasons, will not be encircled by the tetracationic cyclophane.

The design of viable synthetic strategies to prepare the desired [2]catenane **1**·4PF_6 demanded a reevaluation of previous studies (Scheme 1) that focused on the methodology of how to construct mono- and bismacrocycles from TTF units incorporating one or two polyether crown-like moieties. It was believed[6c] (Scheme 1) that distortion of the TTF unit in the bismacrocycle **A** was the reason why catenation of the tetracationic cyclophane $CBPQT^{4+}$ around the HQ unit at room temperature and ambient pressure was prevented. However, in light of the success by which ultrahigh pressure (10 kbar) has been used to facilitate the self-assembly of interlocked structures containing the tetracationic cyclophane $CBPQT^{4+}$ we were encouraged to reexamine if the desired [2]catenane **1**·4PF_6 could in fact be formed under these conditions despite the inherent distortion of the TTF unit.

In this paper we have chosen to employ a bulky macrocyclic TTF derivative[25] as a stepping stone to the construction of a bismacrocyclic compound containing a weak π-electron-donor HQ in the second expanded macrocycle. Subsequently, formation of a [2]catenane by a template-directed synthesis creates a situation where the $CBPQT^{4+}$ cyclophane is left no other choice than to encircle the weaker but readily accessible π-electron donor, i.e., the HQ unit. The linkers between the TTF unit and the HQ moiety were chosen so that they will position the $CBPQT^{4+}$ cyclophane at an ideal distance to be engaged in alongside $\pi-\pi$ interactions with the bulky TTF unit.[6c] This design also allows us to test and eventually refine the hypothesis put forward in the past, namely, that distortion of the TTF unit should actually prevent formation of the tetracationic cyclophane around another π-electron-rich station in the macrocycle. Construction of the [2]catenane such that the $CBPQT^{4+}$ cyclophane can only encircle one of the recognition units also helps to simplify the assignment of both the ^{1}H NMR spectroscopic data and the UV−vis−NIR photophysical data. These assignments serve as signatures that can be utilized in the analysis of more complex interlocked molecules. Through the course of this study the serendipitous crystallization[25] of the *cis* and the *trans* isomers of a protected macrocyclic TTF precursor **5** (Scheme 2) has also allowed for an unambiguous determination of ^{1}H and ^{13}C NMR spectroscopic assignments of the *cis* and *trans* isomers of the TTF-containing bismacrocyclic compound **6** to be carried out. This assignment, in combination with the solid-state structure of the [2]catenane **1**·4PF_6, subsequently allowed us to determine the predominately *cis*-isomer nature of the isolated target [2]catenane. Identification of a single co-conformation of the catenated structure allows us to clearly assign the solution-phase spectroscopic features in the UV−vis−NIR spectra wherein a face-to-face alongside CT interaction leads to strong band intensity while an edge-to-face alongside [Sπ···π] interaction[26] leads to weak band intensity. Resonance Raman spectroscopy has been used to provide an unambiguous assignment of the related absorption band at ~740 nm to the TTF → $CBPQT^{4+}$ CT transition arising from either of the two alongside CT interactions. Taken as a whole, this study provides access to a wide array of heretofore unobtainable catenated structures and detailed spectroscopic assignments.

Results and Discussion

Synthesis. The bismacrocycle **6** was prepared (Scheme 2) by following a convergent synthetic strategy in which the two components, containing either the bulky TTF unit or HQ moiety, were prepared in two separate pathways and then combined in a final step using the pseudo-high-dilution approach. Synthesis

Scheme 1. Previously Attempted Catenation of a Bismacrocycle **A** Containing a Distorted TTF Unit

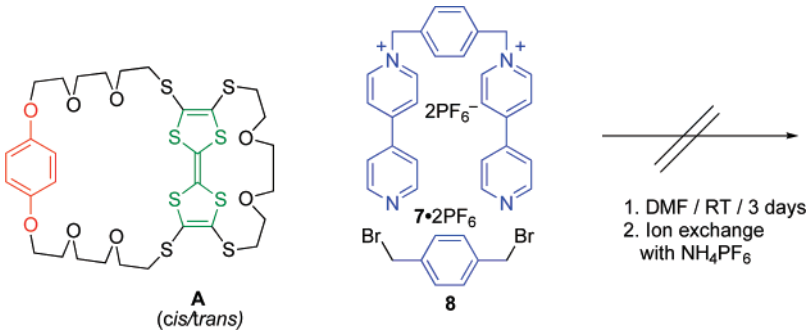

Scheme 2. Synthesis of the HQ-Containing Thread **4** and the Bismacrocyclic Compound **6**

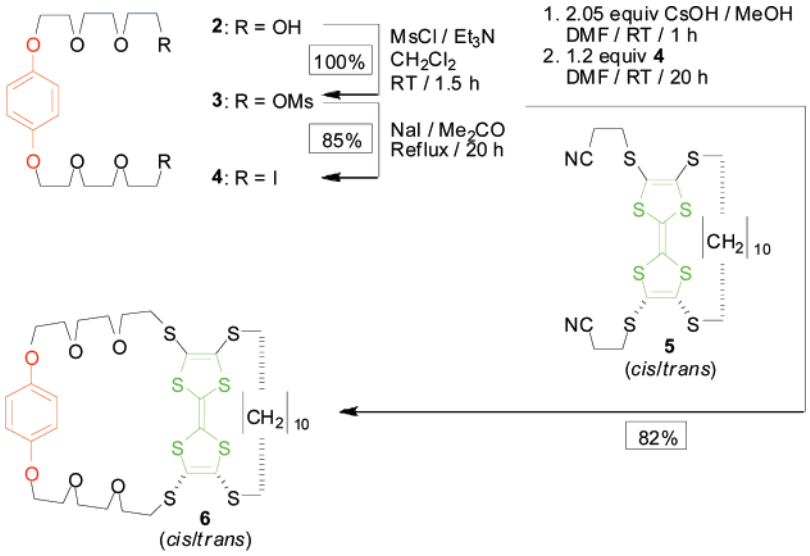

(Scheme 2) of the HQ moiety **4**, which turns out to be a very useful building block for the construction of various interlocked molecules, is not well described in the literature, and the synthetic route was therefore optimized in this study. The dialcohol[27] **2** was mesylated in quantitative yield ($MsCl/Et_3N/CH_2Cl_2$), and a subsequent Finkelstein reaction (NaI/Me_2CO) gave the desired 1,4-bis-{2-[2-(2-iodoethoxy)ethoxy]ethoxy}-benzene (**4**) in good yield (85%).

We previously described[25] the synthesis and full characterization of the bulky TTF macrocycle **5**, and this was used to form (Scheme 2) the bismacrocycle **6** by deprotecting the *cis*/*trans* mixture of the bulky TTF unit **5** in situ using 2.05 equiv of CsOH, whereafter the resulting dithiolate and the HQ-containing diiodo compound **4** were reacted under pseudo-high-dilution conditions in DMF employing a perfusor pump to yield the bismacrocycle **6** in an overall yield of 82%. The initially isolated bismacrocycle **6** was found by ^1H and ^{13}C NMR spectroscopy to exist as a 1:1 mixture of the *cis* and *trans* isomer that could be converted into the predominant *cis* isomer (9:1) by treatment[28] with *p*-toluenesulfonic acid (PTSA) in Me_2CO (see Supporting Information).

The desired [2]catenane **1**·$4PF_6$ was obtained (Scheme 3) from the template-directed high-pressure[29] reaction in DMF where the bismacrocycle **6**, as either the 1:1 or the 9:1 mixture of the *cis*/*trans* isomers, provides the HQ unit as a template around which the $CBPQT^{4+}$ cyclophane forms from its dicationic precursor[15a] **7**·$2PF_6$ and 1,4-bis(bromomethyl)benzene (**8**). In both cases, the [2]catenane **1**·$4PF_6$ was isolated as an analytically pure dark green solid after column chromatography. Starting from the 1:1 *cis*/*trans*-TTF isomeric mixture of **6** a 9% yield of **1**·$4PF_6$ was obtained, whereas **1**·$4PF_6$ was isolated in a 16% yield starting from the 9:1 *cis*/*trans*-TTF isomeric mixture

Scheme 3. Synthesis of the [2]Catenane **1**·$4PF_6$

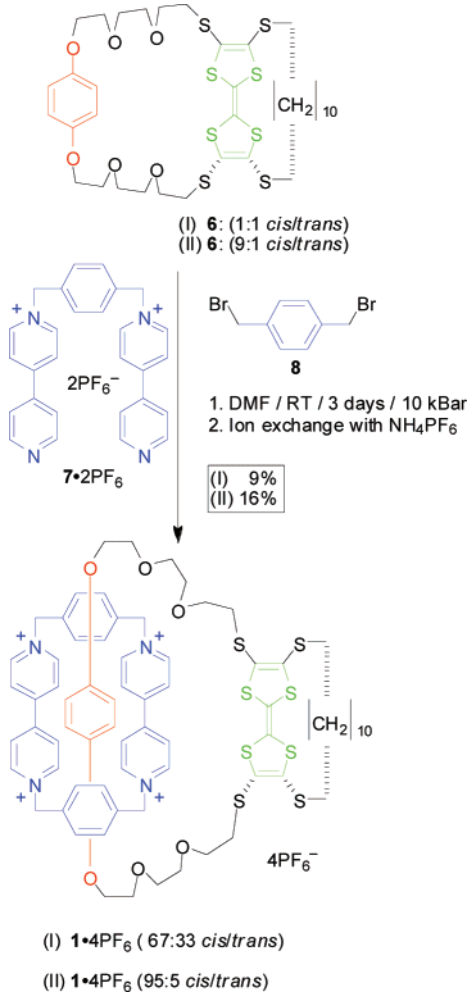

of the bismacrocycle **6**. The observation that the [2]catenane **1**·$4PF_6$ can be isolated in acceptable yields, despite the distortion of the TTF backbone, is in contrast to the previously published assumption[6c] that twisting the TTF backbone totally prevents formation of catenanes. It was initially quite surprising that in both instances the [2]catenane was isolated as a green solid and also produced a green solution upon dissolution. Given the fact

(25) Nygaard, S.; Flood, A. H.; Jeppesen, J. O.; Bond, A. D. *Acta Crystallogr., Sect. C* **2006**, *62*, 677−680.
(26) For an edge-to-face TTF-to-xylene [S···π] interaction of a model host−guest complex, see: Ercolani, G.; Mencarelli, P. *J. Org. Chem.* **2003**, *68*, 6470−6473.
(27) Heilmayer, W.; Wallfisch, B.; Kappe, C. O.; Wentrup, C.; Gloe, K.; Kollenz, G. *Supramol. Chem.* **2003**, *15*, 375−383.
(28) Souizi, A.; Robert, A. *J. Org. Chem.* **1987**, *52*, 1610−1611. (b) Liu, Y.; Flood, A. H.; Moskowitz, R. M.; Stoddart, J. F. *Chem. Eur. J.* **2005**, *11*, 369−385.
(29) Klärner, F.-G.; Wurche, F. *J. Prakt. Chem.* **2000**, *7*, 609−636.

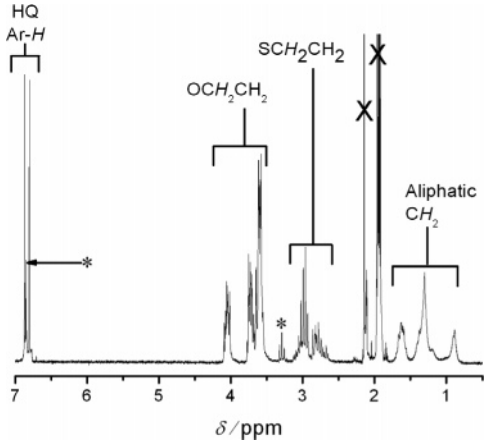

Figure 2. Full ^{1}H NMR (200 MHz) spectrum of the initially isolated *cis*- and *trans*-isomeric mixture of the bismacrocycle **6** recorded in CD_3CN at 298 K. The bismacrocycle is contaminated with the starting diiodo compound **4** as most clearly observed by the signals marked by an asterisk (*).

that the tetracationic cyclophane is forced by the steric bulk of the TTF unit to reside on the HQ unit, a characteristic red color in both the solid state and solution is expected. The green color, therefore, seems to indicate the presence of a moderately strong alongside CT interaction between the TTF unit and one of the bipyridinium moieties of the CBPQT^{4+} cyclophane.

Structural Characterization of the Catenane 1·4PF$_6$ by Mass Spectrometry. The electrospray ionization mass spectrum (ESI-MS) of the [2]catenane **1**·4PF$_6$ shows a diagnostic peak at *m*/*z* 809 corresponding to the doubly charged $[M - 2PF_6]^{2+}$ ion, which unambiguously confirms the presence of the [2]catenane structure.

Structural Characterization of the Bismacrocycle 6 and the [2]Catenane 1·4PF$_6$ by ^{1}H NMR Spectroscopy and X-ray Crystallography. The ^{1}H NMR spectroscopic investigation (Figure 2) of the bismacrocycle **6** carried out in CD_3CN (200 MHz, 298 K) revealed that the initially isolated compound consisted of an approximately 1:1 mixture of the *cis* and *trans* isomers. The most diagnostic evidence supporting this conclusion is the presence of two singlets at $\delta = 6.81$ and 6.87 ppm which originate from the resonances associated with the Ar−*H* protons in the HQ moiety in the *cis* and *trans* isomers of the bismacrocycle **6**, respectively.

The aliphatic region of the ^{1}H NMR spectrum consists of series of multiplets arising from the resonances of the remaining protons in the *cis*/*trans*-isomeric mixture. The multiplets can be categorized into three classes, namely, resonances associated with (i) the C*H*$_2$ protons in the saturated decamethylenedithio linker, (ii) the C*H*$_2$ protons next to an *O* atom, and (iii) the C*H*$_2$ protons next to an *S* atom. Previous[28] investigations have shown that it is possible to alter the *cis*/*trans*-isomeric ratio in TTF derivatives by treatment with PTSA in Me_2CO. A similar isomerization was found to take place in the bismacrocyclic compound **6**, and addition of small amounts of PTSA to a solution (Me_2CO) of the initially 1:1 *cis*/*trans*-isomeric mixture of **6** changed the ratio to approximately 9:1 in favor of the *cis* isomer (for a detailed NMR spectroscopic analysis and assignment of the two TTF isomers, see Supporting Information, Figures S2−S6).

Analysis of the ^{1}H NMR spectrum (CD_3CN, 500 MHz) recorded at 298 K of the green solution of the catenated structure

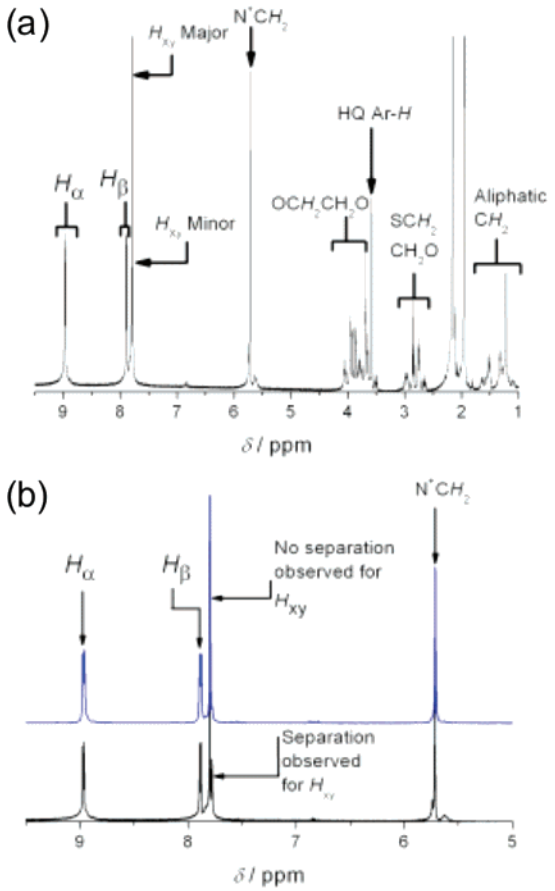

Figure 3. (a) Full ^{1}H NMR spectrum of the [2]catenane **1**·4PF$_6$ (67:33 *cis*/*trans*) obtained from the non-PTSA-treated 1:1 isomeric mixture of the bismacrocycle **6** recorded in CD_3CN (500 MHz) at 298 K. (b) Comparison of the low-field region (9.50−5.00 ppm) of the ^{1}H NMR spectra of the [2]catenane **1**·4PF$_6$ (67:33 *cis*/*trans*) (black solid trace) or the [2]catenane **1**·4PF$_6$ (95:5 *cis*/*trans*) (blue solid trace).

1·4PF$_6$ (Figure 3a), synthesized from the 1:1 *cis*/*trans*-isomeric mixture of the bismacrocycle **6**, unambiguously confirms the presence of the CBPQT^{4+} cyclophane as indicated by two sets of indicative resonances (Figure 3b). These signals correspond to the bipyridinium H_α ($\delta = 8.96$ ppm) and H_β ($\delta = 7.87$ ppm) protons and to the N$^+$C*H*$_2$ protons ($\delta = 5.71$ ppm, singlet) of the cyclophane in the aromatic region of the spectrum. Noteworthy is the appearance of two singlets in varying intensities originating from the resonances associated with the protons in the *p*-phenylene moieties (H_{xy}) ($\delta = 7.79$ and 7.77 ppm) of the tetracationic cyclophane CBPQT^{4+}. The fact that two singlets are observed for the *p*-phenylene moieties indicates[30] that the catenane exists as both the *cis* and the *trans* isomer when synthesized from the 1:1 isomeric mixture of the bismacrocycle **6**. By integration of the area under the two observed H_{xy} signals, the major isomer constitutes 67% of the total population.

On the other hand, when the [2]catenane **1**·4PF$_6$ was synthesized from the PTSA-treated and predominately (9:1) *cis*-

(30) The H_{xy} signal is normally observed as one singlet in the ^{1}H NMR spectrum recorded at room temperature on account of the rotational freedom of the CBPQT^{4+} cyclophane which renders all the H_{xy} protons undistinguishable by ^{1}H NMR spectroscopy. The existence of two H_{xy} signals in **1**·4PF$_6$ with different relative intensities at almost identical positions, therefore, indicates that the H_{xy} experiences two slightly different chemical environments which only can be accounted for by the presence of both a *cis*- and a *trans*-TTF isomer in the isolated [2]catenane **1**·4PF$_6$.

isomeric bismacrocycle **6**, only one singlet ($\delta = 7.79$ ppm) was observed for the protons of the *p*-phenylene moieties of the $CBPQT^{4+}$ cyclophane (Figure 3b). This observation and the overall simplification of the entire spectrum (see Supporting Information, Figure S7) indicate that the isolated [2]catenane **1**·$4PF_6$, when synthesized from a predominately *cis*-isomeric (9:1) macrocycle **6**, is found mainly as a single *cis* isomer (95%) retaining its original stereochemistry. The *cis* isomer was confirmed from an X-ray crystal structure determination (vide infra). This assignment is consistent with the following experimental observations. First, the ^{1}H NMR spectrum of **1**·$4PF_6$ is simpler, displaying fewer resonances, when the [2]catenane is synthesized from the predominately *cis*-isomeric (9:1) bismacrocycle **6** as compared to starting from the 1:1 isomeric mixture of the bismacrocycle **6**. Second, the yield of the high-pressure clipping reaction to form the [2]catenane **1**·$4PF_6$ is observed to almost double from 9% to 16% when the [2]catenane is synthesized from the predominately *cis*-isomeric (9:1) macrocycle **6** as compared to the 1:1 *cis*/*trans*-isomeric mixture of the bismacrocycle **6**. These observations indicate that the template-directed reaction shows isomeric selectivity[31] and predominately takes place around the HQ moiety in the cis isomer of the bismacrocycle **6**.[32] Finally, this is one of a few examples[33] in the literature of a TTF-containing [2]catenane system that is both translational isomer free and where the exact stereochemistry of the isolated compound can be determined unambiguously.

The encirclement of the HQ moiety by the $CBPQT^{4+}$ cyclophane significantly affects the resonance of the aromatic protons on the HQ moiety, and it is evident that these protons have experienced a significant upfield shift as they are now found (Figure 3a) to resonate as a singlet at $\delta = 3.57$ ppm in both the *cis* and *trans* isomers of **1**·$4PF_6$. This new position corresponds to a 3.2 ppm upfield shift of the localization of the HQ protons when compared to the bismacrocycle **6**. No major shifts are observed for the resonances of the SCH_2 protons, but these features are not clearly evident given the multiplet nature and extensive overlap of signals in this region. Nevertheless, these spectroscopic data are entirely consistent with the cyclophane $CBPQT^{4+}$, as expected, exclusively encircling the HQ moiety in the [2]catenane **1**·$4PF_6$, irrespective of its isomeric setup.

Slow diffusion of *i*PrOH into a CD_3CN solution of the [2]catenane **1**·$4PF_6$, obtained from the clipping reaction of the 9:1 *cis*-isomeric bismacrocycle **6** gave orange needle-like crystals suitable for X-ray diffraction analysis.[34] The crystal structure shown in Figure 4 reveals that (i) in the solid state of **1**·$4PF_6$ the tetracationic cyclophane $CBPQT^{4+}$ is positioned around the HQ moiety in accordance with the ^{1}H NMR spectroscopic studies and (ii) the [2]catenane **1**·$4PF_6$ adopts a *cis* configuration. It is noteworthy that the [2]catenane units are arranged in such a way that the TTF unit from one [2]catenane participates in a face-to-face interaction with a TTF unit in a neighboring [2]catenane. By adopting such a face-to-face conformation in the solid state, the TTF units from two different *cis*-[2]catenanes can form favorable ring-over-bond overlap, which is a common feature observed in many crystal structures of TTF derivatives.[35]

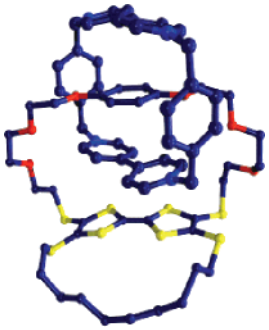

Figure 4. X-ray crystal structure of the *cis* isomer of the [2]catenane **1**·$4PF_6$ depicted as a capped stick representation. Hydrogens, solvent molecules, and counterions are omitted for clarity.

Electrochemical Investigations. Electrochemical investigations were carried out in argon-purged MeCN solutions at room temperature using cyclic voltammetry (CV) and differential pulse voltammetry (DPV). It is well known[36] that TTF can be oxidized reversibly in two discrete steps to the radical cation and the dication. For the bismacrocycle[37] **6** two reversible, monoelectronic oxidation processes associated with the TTF unit are observed in the CV at potentials less than +1.0 V, whereas one reversible two-electron process associated with the oxidation of the HQ moiety is seen (Table 1) at positive potentials greater than +1.0 V. Comparing the electrochemical data of the bismacrocycle **6** to those of the bulky macrocyclic TTF building block[38] **5** reveals that that the presence of cyanoethylthio groups on the TTF unit greatly affects the donor properties of the molecule. As expected, one observes that the TTF unit **5** again is being oxidized in two reversible discrete steps but at significantly higher potential than in the bismacrocycle **6**. This difference is thought to be a result of the presence of two cyanoethylthio groups in **5** which by an inductive process as well as by an internal CT interaction in which the −CN groups receive electrons from the TTF core withdrawing electrons from the TTF unit, thereby decreasing the TTF core's ability to stabilize a positive charge. A better model of the TTF subunit within the bismacrocycle is tetrakis(thiomethyl)TTF **9** (see

(31) For another example of isomeric selectivity in the formation of [2]catenanes, refer to ref 6d.

(32) This assignment is further substantiated and confirmed by the relationship between the observed UV−vis−NIR absorption spectroscopic data and the cis/trans isomer ratio of the [2]catenane as confirmed by molecular modeling.

(33) The exact stereochemistry of a TTF-containing "[2]pseudocatenane" has been reported in refs 6c,d in which the TTF unit, and not the HQ unit, is encircled by the $CBPQT^{4+}$ cyclophane.

(34) Crystallographic data for **1**·$4PF_6$·$(CD_3CN)_7$ at 133(2) K with Mo Kα radiation ($\lambda = 0.71069$ Å). **1**·$4PF_6$: triclinic, space group *P*-1, $a = 13.571(8)$ Å, $b = 14.252(8)$ Å, $c = 27.108(15)$ Å, $\alpha = 97.841(12)°$, $\beta = 91.323(12)°$, $\chi = 106.338(12)°$, $Z = 2$, R1 = 0.0887, wR2 (all data) = 0.2497, GOF = 0.810.

(35) (a) Moore, A. J.; Bryce, M. R.; Cooke, G.; Marshallsay, G. J.; Skabara, P. J.; Batsanov, A. S.; Howard, J. A. K.; Daley, S. T. A. K. *J. Chem. Soc., Perkins Trans.* **1993**, *1*, 1403−1410. (b) Fujiwara, H.; Arai, E.; Kobayashi, H. *J. Mater. Chem.* **1998**, *8*, 829−831. (c) Kimura, S.; Nii, H.; Kurai, H.; Takeuchi, H.; Katsuhara, M.; Mori, T. *Bull. Chem. Soc. Jpn.* **2003**, *76*, 89−96.

(36) (a) Bryce, M. R. *J. Mater. Chem.* **2000**, *10*, 589−598. (b) Segura, J. L.; Martín, N. *Angew. Chem., Int. Ed.* **2001**, *40*, 1372−1409. (c) Schukat, G.; Fanghänel, E. *Sulfur Rep.* **2003**, *24*, 1−190. (d) Becher, J.; Jeppesen, J. O.; Nielsen, K. A. *Synth. Met.* **2003**, *133*−*134*, 309−315. (e) Otsubo, T.; Takimiya, K. *Bull. Chem. Soc. Jpn.* **2004**, *77*, 43−58. (f) Jeppesen, J. O.; Nielsen, M. B.; Becher, J. *Chem. Rev.* **2004**, *104*, 5115−5132. (g) Gorgues, A.; Hudhomme, P.; Sallé, M. *Chem. Rev.* **2004**, *104*, 5151−5184.

(37) No difference in the electrochemical data collected was observed when comparing the electrochemical data of the predominately *cis* isomer (9:1) bismacrocycle **6** to the 1:1 isomeric *cis*/*trans* mixture of the bismacrocycle **6**.

(38) No observable difference in the electrochemical data was observed when the experiments were carried out on either a 1:1 mixture of the *cis* and the *trans* isomer or the purified TTF isomers.

Table 1. Electrochemical Data[a] for the TTF Macrocyclic Compound **5**, Bismacrocycle **6**, Model Compound **9**,[b] and [2]Catenane **1**·4PF_6

compound	bipyridinium[c] E_{red} (V)	TTF E_{ox} (V)		HQ E_{ox} (V)
5		+0.65	+0.90	
6		+0.57	+0.81	+1.35
9		+0.55	*d*	
1·4PF_6	−0.28	+0.65	+0.88	+1.70

[a] Argon-purged MeCN, room temperature, and tetrabutylammmonium hexafluorophosphate (TBAPF_6) as supporting electrolyte. Glassy-carbon working electrode. Potential values are stated in V vs SCE. [b] Compound **9** is a tetrakis(thiomethyl)-substituted TTF derivative (see Supporting Information); data obtained from ref 20 (MeCN, adjusted for SCE from Ag/AgCl). [c] The second reduction process corresponding to the complete reduction of both bipyridinium moieties in the cyclophane, to yield the neutral compound, was observed to be irreversible. [d] Not reported.

Supporting Information),[20] which displays its first oxidation at a position, +0.55 V, that is very similar to **6**, consistent with the equivalent substitution patterns.

It is clearly evident from the electrochemical data of the [2]catenane[39] **1**·4PF_6 that the tetracationic cyclophane does not encircle the TTF unit, but as expected, it encircles the HQ moiety. This gives rise to the very dominant (+350 mV) positive shift of the two-electron process corresponding to oxidation of the HQ moiety inside the cavity of $CBPQT^{4+}$. At a lower positive potential the two processes corresponding to the oxidations of the TTF unit are observed. On account of the close proximity of the tetracationic cyclophane, it is observed that the two TTF-based oxidation processes in **1**·4PF_6 are shifted to higher potential by approximately +80 mV when compared to the same processes in the bismacrocycle **6**. The observed positive shift of the TTF oxidations can be accounted for by the repulsive and through-space electrostatic interactions when the $TTF^{2+/+}$ unit and the $CBPQT^{4+}$ cyclophane are alongside[40] each other. This interpretation is in good agreement with the observed[40] positive shifts previously assigned to similar alongside interactions taking place in bistable [2]pseudorotaxanes. At negative potentials the CV of **1**·4PF_6 exhibits a fully reversible reduction peak, corresponding to the first reduction of both bipyridinium moieties of the cyclophane from the 2+ state to the 1+ state.

Photophysical Investigations and Molecular Modeling of the Alongside Charge-Transfer Interaction. It is well documented[8a,18b−d,20,41] that inclusion of π-electron-rich guests inside the cavity of the tetracationic cyclophane $CBPQT^{4+}$ gives rise to a wealth of [2]pseudorotaxanes in solution as evidenced by the formation of colored solutions and the appearance of characteristic CT bands in the absorption spectra. The location of these CT bands is highly dependent on which guest is being included in the cyclophane. The interaction between TTF derivatives and $CBPQT^{4+}$ is particularly strong, and a large number of [2]pseudorotaxanes have been reported in the literature[20,41] for which it is possible to obtain X-ray crystal structures of some of these superstructures.[42] Notwithstanding all of these instances of CT interactions, there have been few if any UV−vis−NIR absorption studies that specifically[43] probe

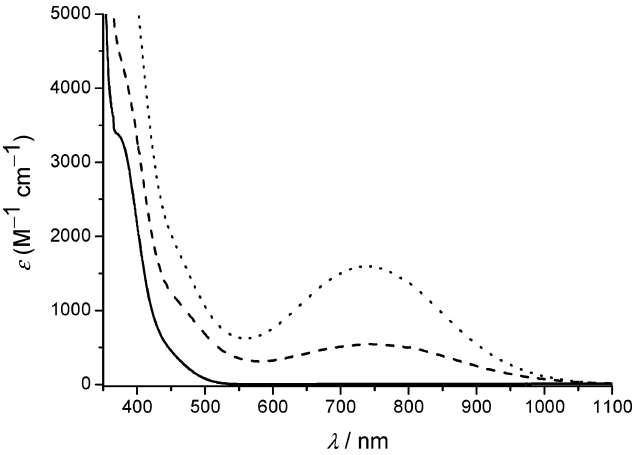

Figure 5. UV−vis−NIR absorption spectrum of the bismacrocycle **6** recorded at room temperature in Me_2CO (solid line), the [2]catenane **1**·4PF_6 (67:33 *cis*/*trans*) in MeCN (dotted line), and the [2]catenane **1**·4PF_6 (95:5 *cis*/*trans*) in MeCN at room temperature (dashed line).

the *alongside* interaction between a TTF unit and the tetracationic cyclophane $CBPQT^{4+}$ in either a [2]pseudorotaxane or a [2]catenane. The chosen molecular design of the [2]catenane **1**·4PF_6 is ideally suited for this purpose. In particular, spectroscopic markers for the situation where the maximum extent of an alongside CT interaction between the TTF unit and the $CBPQT^{4+}$ cyclophane can be realized. Structurally, the flexible PEG chains can accommodate a positioning of the TTF unit approximately 3.5 Å from the cyclophane in order to maximize[6c] the $\pi-\pi$ overlap of the CT interaction.

The absorption spectrum recorded in Me_2CO of the bismacrocyclic compound **6** reveals (Figure 5) an absorption band at 380 nm indicating the presence of a TTF unit. Formation of the [2]catenane **1**·4PF_6 leads to a green-colored solution regardless of the isomeric distribution in the isolated [2]catenane. It is evident from the solution-phase ^1H NMR spectroscopy and CV studies and from the solid-state structure that the tetracationic cyclophane $CBPQT^{4+}$ encircles the HQ unit. Consequently, the green color observed in solution must originate from alongside interactions occurring between the TTF unit and one of the bipyridinium units of the $CBPQT^{4+}$ cyclophane. Inspection of the UV−vis−NIR absorption spectra recorded in MeCN of the two different isomeric mixtures of **1**·4PF_6 reveals the presence of a CT band in the 740 nm region giving rise to the green color. Surprisingly, it can be observed that there is a marked difference in both the location and the intensity of the CT band depending on the *cis*/*trans*-isomeric mixtures. The spectrum recorded of the 67:33 *cis*/*trans* [2]catenane **1**·4PF_6 shows a moderate intensity CT band (ϵ = 1475 M^{-1} s^{-1}) at

(39) No difference in the electrochemical data collected was observed when the [2]catenane (95:5 *cis*/*trans*) prepared from the predominately *cis* isomer (9:1) bismacrocycle **6** or the [2]catenane (67:33 *cis*/*trans*) prepared from a 1:1 isomeric mixture of the bismacrocycle **6** was used in individual experiments.

(40) For a detailed analysis of the electrochemical profile of the alongside interaction in a two-station [2]pseudorotaxane, please refer to refs 18c and 24.

(41) (a) Castro, R.; Nixon, K. R.; Evanseck, J. D.; Kaifer, A. E. *J. Org. Chem.* **1996**, *61*, 9591−9595. (b) Anelli, P.-L. et al. *Chem. Eur. J.* **1997**, *3*, 1113−1135. (c) Ashton, P. R.; Balzani, V.; Becher, J.; Credi, A.; Fyfe, M. C. T.; Mattersteig, G.; Menzer, S.; Nielsen, M. B.; Raymo, F. M.; Stoddart, J. F.; Venturi, M.; Williams, D. J. *J. Am. Chem. Soc.* **1999**, *121*, 3951−3957. (d) Bryce, M. R.; Cooke, G.; Duclairoir, F. M. A.; Rotello, V. M. *Tetrahedron Lett.* **2001**, *42*, 1143−1145.

(42) (a) Philp, D.; Slawin, A. M. Z.; Spencer, N.; Stoddart, J. F.; Williams, D. J. *J. Chem. Soc., Chem. Commun.* **1991**, 1584−1586. (b) Asakawa, M.; Ashton, P. R.; Balzani, V.; Credi, A.; Hamers, C.; Mattersteig, G.; Montalti, M.; Shipway, A. N.; Spencer, N.; Stoddart, J. F.; Tolley, M. S.; Venturi, M.; White, A. J. P.; Williams, D. J. *Angew. Chem., Int. Ed.* **1998**, *37*, 333−337.

(43) The proposed existence of an alongside CT interaction between TTF derivatives and $CBPQT^{4+}$ has been reported in the literature. Please refer to refs 18c and 24. In both cases, the alongside interaction was observed as a weak shoulder in the UV−vis−NIR absorption spectra and arose surreptitously.

740 nm, whereas the spectrum recorded of the 95:5 *cis*/*trans* isomer shows a reduced intensity CT band ($\epsilon = 550\ M^{-1}\ s^{-1}$) at 745 nm. In both cases, a less defined HQ → $CBPQT^{4+}$ CT band at around 475 nm is observed as a shoulder which is consistent[6c,f,g,16a] with the HQ moiety being encircled by the $CBPQT^{4+}$ cyclophane.

It is possible to estimate the intensity of the vis-NIR CT band associated with the wholly *cis* or the *trans* isomer based on the known isomeric distribution in the [2]catenane in the two cases (see Supporting Information). The all-*cis* isomer of **1**·$4PF_6$ would show a weak CT band with an approximate intensity of 380 $M^{-1}\ s^{-1}$, whereas the all-*trans* isomer of **1**·$4PF_6$ would show a strong intensity CT band ($\epsilon = 3690\ M^{-1}\ s^{-1}$). From these experiments it is evident that the configuration of the TTF unit is extremely important for maximizing the alongside CT interaction on account of the 10-fold increase in intensity of the CT band going from the all-*cis* to the all-*trans* TTF isomer of **1**·$4PF_6$. However, based on the crystal structure, wherein the face-to-face TTF-to-$CBPQT^{4+}$ arrangement (i.e., with the TTF oriented face-on to one bipyridinium unit of the $CBPQT^{4+}$ cyclophane) appears optimally suited for a favorable overlap between the TTF-based highest occupied molecular orbital (HOMO) and one of the lowest occupied molecular orbitals (LUMOs) on the $CBPQT^{4+}$ cyclophane, this result is unexpected. Consequently, the difference in overlap between the HOMO on the TTF and one of the LUMOs on the $CBPQT^{4+}$ cyclophane is believed to arise out of the detailed orientation of the two isomers that occur in solution. In support of this interpretation, the crystal structure[25] of the *cis* and *trans* isomers of the macrocycle **5** display very different structures.

To get a better understanding of these observations, we employed molecular modeling to investigate the orientational effects. The conformational space of the *trans*- and *cis*-**1**·$4PF_6$ was investigated by running a 10 ns molecular dynamics simulation using the MMFF force field.[44] Apart from the conformational flexibility of the decamethylenedithio linker, both isomers displayed only one orientation of the TTF and $CBPQT^{4+}$ units during the whole simulation. The *trans* isomer adopts a face-to-face arrangement between the TTF and the $CBPQT^{4+}$ cyclophane, while the *cis* isomer settles into an edge-to-face alignment (see Supporting Information, Figure S9). For each isomer we optimized 1000 structures selected from the 10 ns simulation and reoptimized the lowest energy structure at the B3LYP/6-31G(d) level. These results confirmed that each of the 1000 *trans* isomers is locked in a face-to-face geometry by the constraints of the PEG linker, while the *cis* isomer has substantially more conformational flexibility and prefers to adopt an edge-to-face alignment in all 1000 cases. The latter is in disagreement with the crystal structure, and in order to investigate this discrepancy, we generated two additional starting conformations for the *cis* isomer. One was prepared from the face-to-face *trans* isomer but with the decamethylenedithio linker reconnected into a *cis*-isomeric structure, and a second started from the face-to-face crystal structure. Optimization of both starting geometries at the B3LYP/6-31G(d) level relaxed into the edge-to-face arrangement. We attribute this discrepancy between the observed solid-state conformation and calculated conformations of the *cis* isomer of the [2]catenane $\mathbf{1}^{4+}$ to the presence of crystal-packing forces. In particular, the sum of the favorable ring-over-bond overlap[35] and the face-to-face alongside CT interactions dominate over the edge-to-face CT interaction.

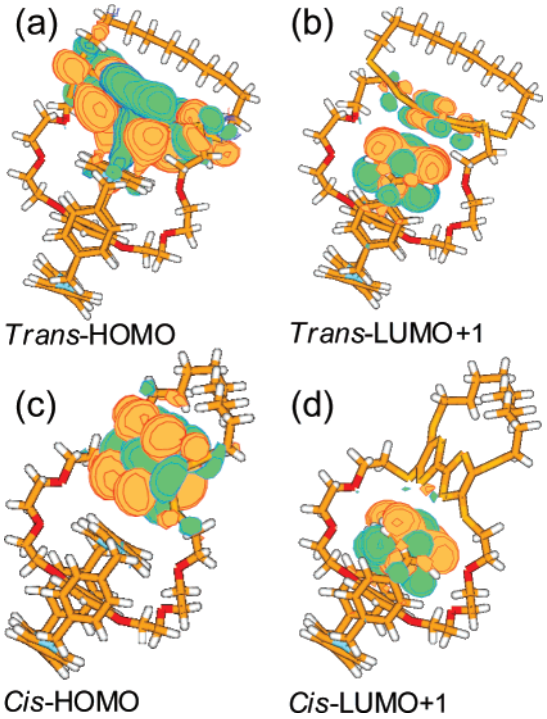

Figure 6. TDHF/6-31G*-generated HOMO (a) and LUMO+1 (b) orbitals for the *trans* isomer of the [2]catenane **1**·$4PF_6$ which shows significant mixing of the orbitals for the *trans* system, whereas the HOMO (c) and LUMO+1 (d) orbitals for the *cis* isomer of the [2]catenane **1**·$4PF_6$ shows that the molecular orbitals are localized in this case.

With the calculated *cis*- and *trans*-isomeric structures as a starting point, we investigated the electronic features of the alongside CT interaction. From TDHF/6-31G(d) calculations performed on both [2]catenanes, the LUMO is actually located on the bipyridinium furthest away, leaving the LUMO+1 available for the CT interaction For the *cis* isomer, a small degree (16%) of mixing (defined as the overlap of the orbital charge densities) is present[45] between the HOMO localized on the TTF unit and the LUMO+1 localized on the $CBPQT^{4+}$ cyclophane when it adopts the edge-to-face conformation, whereas significant mixing (34%) of the HOMO and LUMO+1 is observed for the *trans* isomer (Figure 6) in the face-to-face conformation. From the excitation energy calculations the oscillator strength of the predominately HOMO → LUMO+1 transition is roughly five times larger for the *trans* system than the *cis* system, which is in agreement with the experimentally observed UV−vis−NIR absorption spectroscopic behavior of the *trans* isomer compared to the *cis* isomer of the [2]rotaxane **1**·$4PF_6$. The calculated CT band position is predicted to be at somewhat shorter wavelength for the *trans* isomer (707 nm) compared to the *cis* isomer (774 nm), which again matches the trend for the observed difference in location of the CT bands found in solution at 740 and 745 nm for the (67:23 *cis*/*trans*) **1**·$4PF_6$ and the (95:5 *cis*/*trans*) **1**·$4PF_6$, respectively. From these calculations, we infer that the *trans*-**1**·$4PF_6$ catenane has a stable face-to-face conformation that produces the intense alongside

(44) Jensen, F. *Introduction to Computational Chemistry*, 2nd edition; VCH-Wiley: Chichester, 2006.

(45) Lee, E. C.; Hong, H.; Lee, J. Y.; Kim, J. C.; Kim, D.; Kim, Y.; Tarakeshwar, P.; Kim, K. S. *J. Am. Chem. Soc.* **2005**, *127*, 4530−4537.

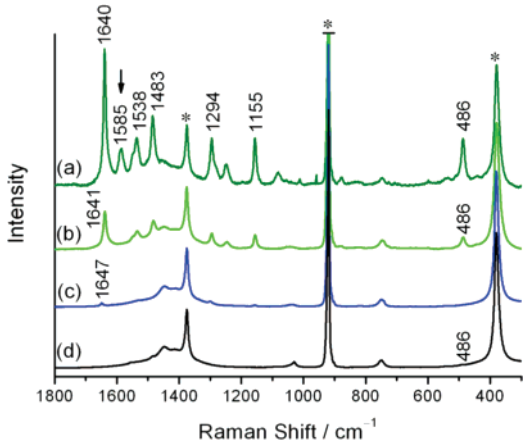

Figure 7. Raman spectroscopic data of a MeCN solution (4.5 mM) of the (a) 67:33 *cis*/*trans* [2]catenane **1**·4PF$_6$, (b) 95:5 *cis*/*trans* [2]catenane **1**·4PF$_6$, (c) **CBPQT**$^{4+}$, and (d) 1:1 *cis*/*trans* isomer mixture of the bismacrocycle **6**. MeCN features as marked by an asterisk (*).

CT absorption band. By contrast, the *cis* form of the catenane derives its weakened CT intensity from poorer HOMO → LUMO+1 overlap of the edge-to-face conformation. This arrangement determines that one of the sulfur atoms in the TTF unit lies above the center of a pyridinium ring at a distance of 3.67 Å and the other sulfur is situated above the interring carbon of the adjacent pyridinium ring at a distance of 3.72 Å. This relative orientation in the *cis* isomer corresponds to a [Sπ···π] CT interaction arising from the small degree of π-orbital overlap. The contribution of the [Sπ···π] CT interaction to host−guest complexation has been described computationally[26] for the TTF-to-xylene orientation in a model complex with CBPQT^{4+}. Finally, we believe that this [Sπ···π] CT interaction does not contribute significantly to the total sum of the noncovalent bonding interactions—it has weak CT band intensity and its influence on structure can be overturned in the solid state.

Structural Characterization of the Model Compounds and the Catenane 1·4PF$_6$ by Resonance Raman Spectroscopy. In order to verify that the band at ∼740 nm is a TTF → CBPQT^{4+} transition arising from an alongside interaction, the resonance Raman spectra of the two isomer distributions of the [2]catenane **1**·4PF$_6$ were recorded and compared to the Raman spectra of model compounds **6** and **CBPQT**$^{4+}$. When the laser excitation wavelength (λ_{exc}) is selected such that it comes into resonance with a molecular chromophore two features of the resulting resonance Raman spectra allow for the nature of the electronic transition to be assigned.[46] First, the spectrum's signal intensity becomes resonantly enhanced. Second, the specific vibrational bands that gain intensity by the resonance effect are chromophore specific and therefore, directly correspond to the donor and acceptor molecular orbitals. The 740 nm band is assigned to a HOMO(TTF) → LUMO^{+1}(CBPQT^{4+}) electronic transition. Laser excitation within the absorption profile (λ_{exc} = 785 nm) is therefore expected to selectively enhance[47] (Figure 7) diagnostic bands attributed to the TTF unit[48] and the CBPQT^{4+} cyclophane,[49] as observed.

Compared to the solution-phase Raman spectra (MeCN, Figure 7) of the individual components of the [2]catenane, i.e., the bismacrocycle **6** and the tetracationic cyclophane **CBPQT**$^{4+}$, the spectra of both isomeric ratios of the [2]catenane **1**·4PF$_6$ display strong resonantly enhanced spectra. For example, the CBPQT^{4+}-based marker band at ∼1640 cm^{-1} is enhanced 6-fold for the 95:5 *cis*/*trans* [2]catenane **1**·4PF$_6$, whereas a remarkable 30-fold enhancement is seen for the 67:33 *cis*/*trans* [2]catenane **1**·4PF$_6$ when utilizing the MeCN 919 cm^{-1} band as an internal standard (see Supporting Information, Table S2). All of the remaining bands are resonantly enhanced to a similar degree. One band that can definitively be assigned to the TTF unit in the 95:5 *cis*/*trans* sample of the [2]catenane **1**·4PF$_6$ is the C═C interring stretch at 486 cm^{-1}, displaying a significantly large enhancement compared to the spectrum of the bismacrocycle **6**. This band is also seen to be enhanced strongly in the 67:33 *cis*/*trans* [2]catenane **1**·4PF$_6$. The greater degree of intensity enhancement of the entire spectrum in the latter isomeric ratio corresponds to the larger molecular absorptivity observed in the UV−vis−NIR absorption spectrum for the 67:33 *cis*/*trans* sample of the [2]catenane **1**·4PF$_6$. In order to verify the chromophore-specific spectrum for the TTF → CBPQT^{4+} CT transition, the same spectra for a model TTF unit **9** and the associated [2]pseudorotaxane **9**⊂**CBPQT**$^{4+}$ have been recorded (see Supporting Information, Scheme S1 and Figure S10). All of the important features are retained, and a ∼5-fold enhancement of the CBPQT^{4+} marker band and the $\nu_{C=C}$ TTF interring band are observed for the [2]pseudorotaxane. While the overall degree of enhancement appears to follow the difference in extinction coefficient of each sample, one new band is observed at 1585 cm^{-1} (arrow in Figure 7a) in the 67:33 *cis*/*trans* isomer. This band is not seen in the model TTF system **9**, which does not have any isomers, therefore implying that the C_{2h} microsymmetry of the *trans* isomer allows for one additional Raman-active vibrational mode to gain intensity compared with the C_{2v} *cis* isomer. Consistent with the CT interaction and the mixing of the CBPQT^{4+} LUMO+1 into the occupied HOMO, the ∼1647 cm^{-1} marker band of CBPQT^{4+} has shifted down in energy by 7 cm^{-1}. This shift is attributed to the CT interaction with the TTF unit and not with the HQ moiety on account of the fact that the CT band intensity of the former far exceeds the latter and that the marker band does not shift position when the CBPQT^{4+} cyclophane is threaded with the HQ moiety **2** (see Supporting Information, Figure S11). Surprisingly, the TTF-based band at 486 cm^{-1} does not shift due to the CT interaction. It is important to note that the impact of the alongside CT interaction is observed most acutely in the photophysical properties (UV−vis−NIR and Raman spectroscopy) compared with either ^{1}H NMR spectroscopy or electrochemistry. This brings out an important comment that when alongside TTF → CBPQT^{4+} CT interactions are playing a role in influencing distributions of co-conformations, one would expect to detect this band by the presence of the CT chromophore in the UV−vis−NIR spectrum and/or through the chromophore-specific resonance Raman spectrum.

Conclusion

We have demonstrated that it is possible to synthesize a [2]catenane **1**·4PF$_6$ wherein the cyclophane component

(46) Hirakawa, A. Y.; Tsuboi, M. *Science* **1975**, *188*, 359−361.
(47) Flood, A. H.; Wong, E. W.; Stoddart, J. F. *Chem. Phys.* **2006**, *324*, 280−290.
(48) Joy, V. T.; Srinivasan, T. K. K. *Chem. Phys. Lett.* **2000**, *328*, 221−226.
(49) (a) Lee, P. C.; Schmidt, K.; Gordon, S.; Meisel, D. *Chem. Phys. Lett.* **1981**, *80*, 242−249. (b) Hennessy, B.; Megelski, S.; Marcolli, C.; Shklover, V.; Bärlocher, C.; Calzaferri, G. *J. Phys. Chem. B.* **1999**, *103*, 3340−3351.

$CBPQT^{4+}$ is forced to reside on the weakest π-electron donor by employing a bulky and distorted TTF unit that does not fit inside the cavity of the $CBPQT^{4+}$ cyclophane. Furthermore, we demonstrated that it is possible to optimize the yield by utilizing the *cis*/*trans* stereoselectivity of the high-pressure clipping reaction leading to the [2]catenane. Bearing in mind that the tetracationic cyclophane is found exclusively to encircle the HQ moiety, it was quite surprising to find for both samples of the [2]catenane **1**·$4PF_6$ that the alongside CT band at ∼740 nm dominates over the CT band originating from the HQ → $CBPQT^{4+}$ transition at 475 nm to such an extent that a green color is observed in solution instead of the expected red solution. Furthermore, the position and intensity of the alongside CT band assigned to the TTF → $CBPQT^{4+}$ transition is strongly dependent on the *cis*/*trans* configuration of the TTF unit. Molecular dynamics and electronic structure calculations allowed us to distinguish between a single low-energy face-to-face conformation of the *trans* isomer and an edge-to-face arrangement for the *cis* isomer, which defines a weak [Sπ···π] CT interaction. The *trans* isomer, with a high degree of HOMO-(TTF)-to-LUMO+1($CBPQT^{4+}$) overlap, contrasts well with the smaller overlap for the *cis* isomer. Employing the incisive concept of resonance Raman spectroscopy allowed us to unambiguously assign the 740 nm band to the TTF → $CBPQT^{4+}$ transition of the alongside CT interaction on account of the selective enhancement of diagnostic bands of the TTF unit and the $CBPQT^{4+}$ cyclophane. In conclusion, our findings indicate that a weaker CT interaction based on a [Sπ···π] edge-to-face arrangement can be identified in instances when the more common face-to-face orientation is structurally eliminated.

Acknowledgment. This work was funded in part by a Ph.D. Scholarship from the University of Southern Denmark to S.N., the Danish Natural Science Research Council (SNF, project #21-03-0317), the Danish Strategic Research Council in Denmark through the Young Researchers Programme (#2117-05-0115), and the Danish Center for Scientific Computing.

Supporting Information Available: Synthetic procedure of all compounds as well as relevant NMR spectroscopic data, X-ray crystal data details, UV−vis−NIR absorption spectra, modeling details, and Raman spectroscopic data. This material is available free of charge via the Internet at http://pubs.acs.org.

JA069047W